

Supplementary Materials: Improved co-registration of Sentinel-2 and Landsat-8 imagery for Earth surface motion measurements

André Stumpf ^{1,*}, David Michéa ^{1,2} and Jean-Philippe Malet ^{1,3}

1. Datasets

Table S1. List of Sentinel-2 and Landsat-8 scenes used for the evaluation of the co-registration precision with the master images in **bold** font.

USA 14 SKF	
Scene identifier	
S2A_MSIL1C_20160112T174916_N0201_R055_T14SKF_20160113T013403	
S2A_MSIL1C_20160211T174108_N0201_R055_T14SKF_20160212T010507	
S2A_MSIL1C_20160312T173504_N0201_R055_T14SKF_20160313T010958	
S2A_MSIL1C_20160511T174344_N0202_R055_T14SKF_20160512T065256	
LC80310342015245LGN00	
LC80310342015261LGN00	
LC80310342015293LGN00	
LC80310342015309LGN00	
LC80310342015325LGN00	
LC80310342015341LGN00	
LC80310342015357LGN00	
LC80310342016024LGN00	
LC80310342016040LGN00	
LC80310342016056LGN00	
LC80310342016072LGN00	
LC80310342016088LGN00	
LC80310342016104LGN00	
LC80310352015245LGN00	
LC80310352015261LGN00	
LC80310352015293LGN00	
LC80310352015309LGN00	
LC80310352015325LGN00	
LC80310352015341LGN00	
LC80310352015357LGN00	
LC80310352016024LGN00	
LC80310352016040LGN00	
LC80310352016056LGN00	
LC80310352016072LGN00	
LC80310352016088LGN00	
LC80310352016104LGN00	
Argentina 20HNH	
Scene identifier	
S2A_MSIL1C_20151224T141244_N0201_R067_T20HNH_20151224T202609	
S2A_MSIL1C_20151207T142112_N0204_R110_T20HNH_20170527T235150	

S2A_MSIL1C_20160106T142247_N0201_R110_T20HNNH_20160107T001430
 S2A_MSIL1C_20160113T141828_N0201_R067_T20HNNH_20160113T224027
 S2A_MSIL1C_20160116T142245_N0201_R110_T20HNNH_20160117T090904
 S2A_MSIL1C_20160123T141248_N0201_R067_T20HNNH_20160125T105737
 S2A_MSIL1C_20160126T142112_N0201_R110_T20HNNH_20160128T123541
 S2A_MSIL1C_20160212T140814_N0201_R067_T20HNNH_20160213T004942
 S2A_MSIL1C_20160215T142143_N0201_R110_T20HNNH_20160215T234927
 S2A_MSIL1C_20160303T141102_N0201_R067_T20HNNH_20160305T130123
 S2A_MSIL1C_20160313T140130_N0201_R067_T20HNNH_20160313T222921
 S2A_MSIL1C_20160313T141151_N0201_R067_T20HNNH_20160313T230452
 S2A_MSIL1C_20160323T141104_N0201_R067_T20HNNH_20160323T231257
 S2A_MSIL1C_20160402T141105_N0201_R067_T20HNNH_20160403T125536

LC82270832015242LGN00

LC82270832015290LGN00

LC82270832015338LGN00

LC82270832015354LGN00

LC82270832016021LGN00

LC82270842015338LGN00

LC82270842016053LGN00

LC82280832015329LGN01

LC82280832015345LGN00

LC82280832015361LGN00

LC82280842015185LGN00

LC82280842015201LGN00

LC82280842015329LGN01

LC82280842015361LGN00

LC82270832015258LGN00

LC82270832015306LGN00

LC82270832016037LGN00

LC82270832016053LGN00

LC82270842015242LGN00

LC82270842015258LGN00

LC82270842015290LGN00

LC82270842015306LGN00

LC82270842015354LGN00

LC82270842016021LGN00

LC82270842016037LGN00

LC82280832015185LGN00

LC82280832015201LGN00

LC82280832015249LGN00

LC82280842015249LGN00

LC82280842015345LGN00

Argentina 20HPH

Scene identifier

S2A_MSIL1C_20151224T141244_N0201_R067_T20HPH_20151224T202609

S2A_MSIL1C_20160113T141828_N0201_R067_T20HPH_20160113T224027

S2A_MSIL1C_20160123T141248_N0201_R067_T20HPH_20160125T105737

S2A_MSIL1C_20160212T140814_N0201_R067_T20HPH_20160213T004942

S2A_MSIL1C_20160303T141102_N0201_R067_T20HPH_20160305T130123

S2A_MSIL1C_20160313T141151_N0201_R067_T20HPH_20160313T230452
 S2A_MSIL1C_20160323T141104_N0201_R067_T20HPH_20160323T231257
 S2A_MSIL1C_20160402T141105_N0201_R067_T20HPH_20160403T125536
 LC82270832015242LGN00
 LC82270832015258LGN00
 LC82270832015290LGN00
 LC82270832015306LGN00
 LC82270832015338LGN00
 LC82270832015354LGN00
 LC82270832016021LGN00
 LC82270832016037LGN00
 LC82270832016053LGN00
 LC82270842015242LGN00
 LC82270842015258LGN00
 LC82270842015290LGN00
 LC82270842015306LGN00
 LC82270842015338LGN00
 LC82270842015354LGN00
 LC82270842016021LGN00
 LC82270842016037LGN00
 LC82270842016053LGN00

Ukraine 34UFU

Scene identifier

S2A_MSIL1C_20160217T093042_N0201_R136_T34UFU_20160217T163527
S2A_MSIL1C_20160716T093411_N0204_R136_T34UFU_20160716T145454
 S2A_MSIL1C_20160726T093038_N0204_R136_T34UFU_20160726T21085
 LC81850262016063LGN00
 LC81850272016063LGN00
 LC81860262016182LGN00
 LC81860272016182LGN00

Ukraine 36UUU

Scene identifier

S2A_MSIL1C_20160405T085012_N0201_R107_T36UUU_20160407T042952
 S2A_MSIL1C_20160418T090432_N0201_R007_T36UUU_20160418T170647
 S2A_MSIL1C_20160428T090022_N0201_R007_T36UUU_20160428T165323
 S2A_MSIL1C_20160604T085207_N0202_R107_T36UUU_20160708T173450
 S2A_MSIL1C_20160614T085018_N0202_R107_T36UUU_20160614T161101
S2A_MSIL1C_20160617T090020_N0204_R007_T36UUU_20160618T074301
 S2A_MSIL1C_20160627T090349_N0204_R007_T36UUU_20160627T183540
 S2A_MSIL1C_20160714T085152_N0204_R107_T36UUU_20160714T144734
 S2A_MSIL1C_20160717T090142_N0204_R007_T36UUU_20160717T201927
 S2A_MSIL1C_20160724T085019_N0204_R107_T36UUU_20160724T142347
 LC81800262016076LGN00
 LC81800262016092LGN00
 LC81800262016108LGN00
 LC81800262016156LGN00
 LC81800262016172LGN00

LC81800262016188LGN00
 LC81800272016076LGN00
 LC81800272016092LGN00
 LC81800272016108LGN00
 LC81800272016156LGN00
 LC81800272016172LGN00
 LC81800272016188LGN00

Table S2. List of Sentinel-2 and Landsat-8 scenes used for the evaluation of the co-registration precision with the master images in **bold font**.

South Africa	
Scene identifier	Tile identifier
S2A_OPER_PRD_MSIL1C_PDMC_20170602T040635_R135_V20151209T075322_20151209T075322	S2A_OPER_MSI_L1C_TL_EPA_20170601T200034_A002420_T35JPN_N02.04
	S2A_OPER_MSI_L1C_TL_EPA_20170601T200034_A002420_T35JQN_N02.04
LC81700772015339LGN00	
S2A_OPER_PRD_MSIL1C_PDMC_20151218T181852_R121_V20151218T085036_20151218T085036	S2A_OPER_MSI_L1C_TL_SGS_20151218T140504_A002549_T34HBJ_N02.01
S2A_OPER_PRD_MSIL1C_PDMC_20170530T013237_R121_V20151208T082332_20151208T082332	S2A_OPER_MSI_L1C_TL_EPA_20170529T222118_A002406_T34HBJ_N02.04
LC81750832015326LGN00	
S2A_OPER_PRD_MSIL1C_PDMC_20151218T181852_R121_V20151218T085036_20151218T085036	S2A_OPER_MSI_L1C_TL_SGS_20151218T140504_A002549_T34HBH_N02.01
S2A_OPER_PRD_MSIL1C_PDMC_20170530T013237_R121_V20151208T082332_20151208T082332	S2A_OPER_MSI_L1C_TL_EPA_20170529T222118_A002406_T34HBH_N02.04
LC81750842015326LGN00	

Table S3. List of Sentinel-2 images used to evaluate the stability of the co-registration accuracy over time with the master images in **bold font**.

Scene identifier
S2A_MSIL1C_20160505T103027_N0202_R108_T31T GK_20160505T205953
S2A_MSIL1C_20160515T103028_N0202_R108_T31T GK_20160516T015231
S2A_MSIL1C_20160528T104248_N0202_R008_T31T GK_20160528T223627
S2A_MSIL1C_20160624T103721_N0204_R108_T31T GK_20160624T193752
S2A_MSIL1C_20160627T104023_N0204_R008_T31T GK_20160627T212648
S2A_MSIL1C_20160707T104025_N0204_R008_T31T GK_20160707T174208
S2A_MSIL1C_20160717T104026_N0204_R008_T31T GK_20160718T061224
S2A_MSIL1C_20160803T103724_N0204_R108_T31T GK_20160805T220539
S2A_MSIL1C_20160813T103022_N0204_R108_T31T GK_20160814T185238
S2A_MSIL1C_20160816T104022_N0204_R008_T31T GK_20160816T231309
S2A_MSIL1C_20160823T103022_N0204_R108_T31T GK_20160824T205632
S2A_MSIL1C_20160826T104022_N0204_R008_T31T GK_20160827T194742
S2A_MSIL1C_20160902T103022_N0204_R108_T31T GK_20160903T181623
S2A_MSIL1C_20160922T103022_N0204_R108_T31T GK_20160924T025011
S2A_MSIL1C_20160925T104022_N0204_R008_T31T GK_20160926T220949
S2A_MSIL1C_20161005T104022_N0204_R008_T31T GK_20161005T213407
S2A_MSIL1C_20161015T104022_N0204_R008_T31T GK_20161016T190406
S2A_MSIL1C_20161022T103052_N0204_R108_T31T GK_20161022T224014
S2A_MSIL1C_20161101T103202_N0204_R108_T31T GK_20161101T190224
S2A_MSIL1C_20161201T103412_N0204_R108_T31T GK_20161201T210307
S2A_MSIL1C_20161204T104422_N0204_R008_T31T GK_20161204T170703
S2A_MSIL1C_20161211T103432_N0204_R108_T31T GK_20161211T103426
S2A_MSIL1C_20161214T104432_N0204_R008_T31T GK_20161214T104609
S2A_MSIL1C_20161231T103432_N0204_R108_T31T GK_20161231T103428
S2A_MSIL1C_20170219T103051_N0204_R108_T31T GK_20170219T103333
S2A_MSIL1C_20170311T103011_N0204_R108_T31T GK_20170311T103014
S2A_MSIL1C_20170314T104011_N0204_R008_T31T GK_20170314T104411
S2A_MSIL1C_20170321T103011_N0204_R108_T31T GK_20170321T103014
S2A_MSIL1C_20170403T104021_N0204_R008_T31T GK_20170403T104138
S2A_MSIL1C_20170410T103021_N0204_R108_T31T GK_20170410T103020
S2A_MSIL1C_20170423T104021_N0204_R008_T31T GK_20170423T104254
S2A_MSIL1C_20170602T104021_N0205_R008_T31T GK_20170602T104212
S2A_MSIL1C_20170612T104021_N0205_R008_T31T GK_20170612T104258
S2A_MSIL1C_20170619T103021_N0205_R108_T31T GK_20170619T103806
S2A_MSIL1C_20170622T104021_N0205_R008_T31T GK_20170622T104021
S2A_MSIL1C_20170722T104021_N0205_R008_T31T GK_20170722T104522
S2A_MSIL1C_20170818T103021_N0205_R108_T31T GK_20170818T103421
S2A_MSIL1C_20170821T104021_N0205_R008_T31T GK_20170821T104208

Table S4. List of Sentinel-2 images used for the analysis of the surface displacement of the Harmalière landslide / French Alps.

Scene identifier
S2A_MSIL1C_20160505T103027_N0202_R108_T31TGG_20160505T205953
S2A_MSIL1C_20160515T103028_N0202_R108_T31TGG_20160516T015231
S2A_MSIL1C_20160528T104248_N0202_R008_T31TGG_20160528T223627
S2A_MSIL1C_20160624T103721_N0204_R108_T31TGG_20160624T193752
S2A_MSIL1C_20160627T104023_N0204_R008_T31TGG_20160627T212648
LC81960292016188LGN00
S2A_MSIL1C_20160707T104025_N0204_R008_T31TGG_20160707T174208
S2A_MSIL1C_20160717T104026_N0204_R008_T31TGG_20160718T061224
S2A_MSIL1C_20160803T103724_N0204_R108_T31TGG_20160805T220539
S2A_MSIL1C_20160813T103022_N0204_R108_T31TGG_20160814T185238
S2A_MSIL1C_20160816T104022_N0204_R008_T31TGG_20160816T231309
S2A_MSIL1C_20160823T103022_N0204_R108_T31TGG_20160824T205632
S2A_MSIL1C_20160826T104022_N0204_R008_T31TGG_20160827T194742
S2A_MSIL1C_20160902T103022_N0204_R108_T31TGG_20160903T181623
S2A_MSIL1C_20160922T103022_N0204_R108_T31TGG_20160924T025011
S2A_MSIL1C_20160925T104022_N0204_R008_T31TGG_20160926T220949
S2A_MSIL1C_20161015T104022_N0204_R008_T31TGG_20161016T190406
S2A_MSIL1C_20161022T103052_N0204_R108_T31TGG_20161022T224014
S2A_MSIL1C_20161101T103202_N0204_R108_T31TGG_20161101T190224
S2A_MSIL1C_20161201T103412_N0204_R108_T31TGG_20161201T210307
S2A_MSIL1C_20161211T103432_N0204_R108_T31TGG_20161211T103426
S2A_MSIL1C_20161231T103432_N0204_R108_T31TGG_20161231T103428
S2A_MSIL1C_20170219T103051_N0204_R108_T31TGG_20170219T103333
S2A_MSIL1C_20170311T103011_N0204_R108_T31TGG_20170311T103014
S2A_MSIL1C_20170314T104011_N0204_R008_T31TGG_20170314T104411
S2A_MSIL1C_20170403T104021_N0204_R008_T31TGG_20170403T104138
S2A_MSIL1C_20170423T104021_N0204_R008_T31TGG_20170423T104254
S2A_MSIL1C_20170602T104021_N0205_R008_T31TGG_20170602T104212
S2A_MSIL1C_20170612T104021_N0205_R008_T31TGG_20170612T104258
S2A_MSIL1C_20170622T104021_N0205_R008_T31TGG_20170622T104021
S2A_MSIL1C_20170722T104021_N0205_R008_T31TGG_20170722T104522
S2A_MSIL1C_20170821T104021_N0205_R008_T31TGG_20170821T104208

Table S5. List of Sentinel-2 images used to assess the surface displacement linked to the co-seismic slip of the Kaikoura earthquake / New Zealand.

Before
Scene identifier
S2A_OPER_PRD_MSIL1C_PDMC_20160101T024957_R029_V20151231T222846_20151231T222846
S2A_OPER_PRD_MSIL1C_PDMC_20160530T024210_R029_V20160529T222549_20160529T222549
S2A_OPER_PRD_MSIL1C_PDMC_20160914T022139_R129_V20160913T221602_20160913T221629
S2A_OPER_PRD_MSIL1C_PDMC_20161004T005110_R129_V20161003T221602_20161003T221657
After
Scene identifier
S2A_OPER_PRD_MSIL1C_PDMC_20161123T010941_R129_V20161122T221602_20161122T221602
S2A_OPER_PRD_MSIL1C_PDMC_20161206T190951_R029_V20161205T222542_20161205T222542
S2A_MSIL1C_20161215T222542_N0204_R029_T59GQP_20161215T222539
S2A_MSIL1C_20170223T222531_N0204_R029_T59GQP_20170223T222726
S2A_MSIL1C_20170504T222541_N0205_R029_T59GQP_20170504T222620

2. Outlier removal

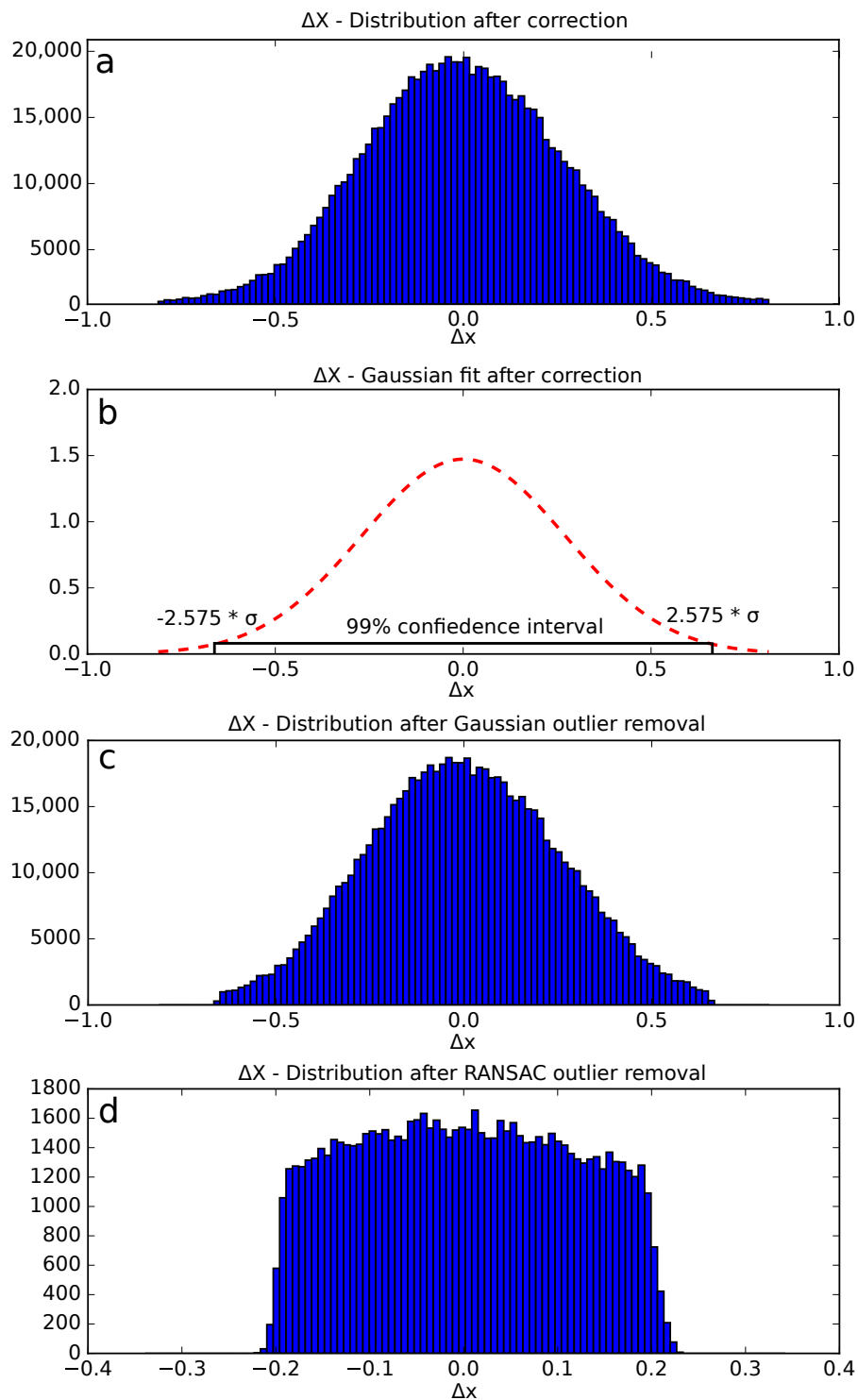


Figure S1. Comparison of removing outliers from (a) corrected displacement measurements. Using (b) a Gaussian fit with 99% confidence leads to (c) a much more conservative distribution than when using RANSAC (d) with 99% confidence interval and 100 iterations which removes the upper and lower tails drastically.

3. Fault slip

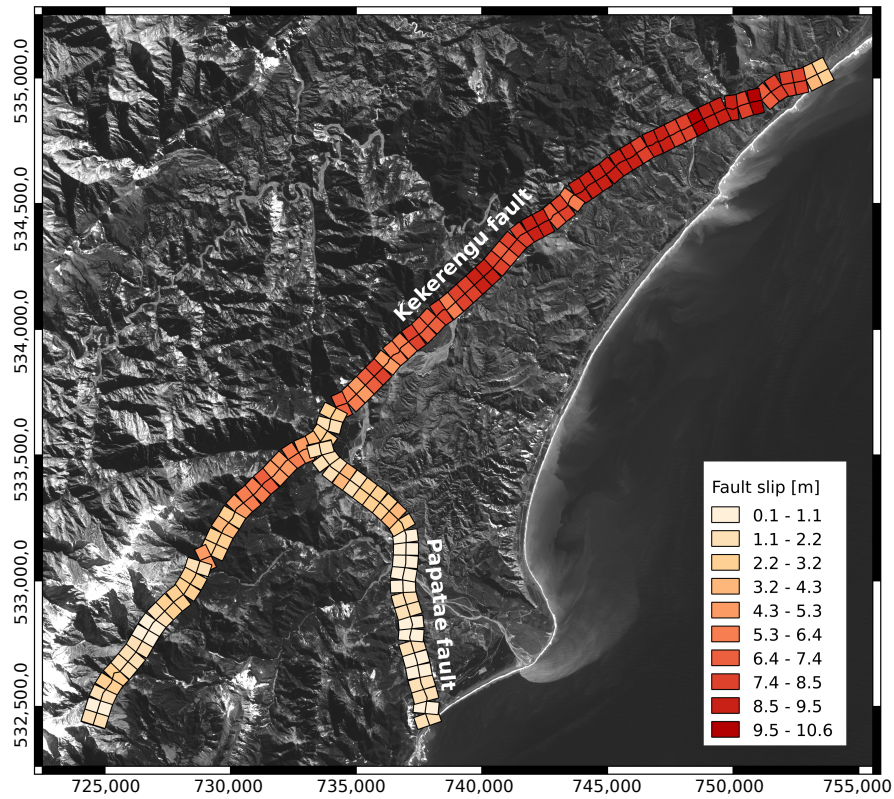


Figure S2. Horizontal co-seismic surface slip along the Kekerengu and Papatae faults derived from the projection of the measured displacements along the bearing of the faults. The total slip is computed as the difference of the medians on both sides of the fault.